Indium–carbon pairs in germanium

2003 J. Phys.: Condens. Matter 15 5297

(http://iopscience.iop.org/0953-8984/15/30/311)

INSTITUTE OF PHYSICS PUBLISHING JOURNAL OF PHYSICS: CONDENSED MATTER

J. Phys.: Condens. Matter **15** (2003) 5297–5306 PII: S0953-8984(03)61579-1

Indium–carbon pairs in germanium

G Tessema and R Vianden

Helmholtz Institut für Strahlen- und Kernphysik, Universität Bonn, Nussallee 14-16, 53115 Bonn, Germany

E-mail: tessema@iskp.uni-bonn.de

Received 1 April 2003, in final form 11 June 2003
Published 18 July 2003
Online at stacks.iop.org/JPhysCM/15/5297

Abstract

The interactions of carbon with the probe nucleus ^{111}In have been studied in germanium using the perturbed angular correlation method, which has the ability to detect the microscopic environments of the probe atom by means of the interaction of the nuclear moments of the probe with the surrounding electromagnetic fields. At high dose carbon implantation in germanium two complexes have been identified by their unique quadrupole interaction frequencies. An interaction frequency of $\nu_{Q1} = 207(1)$ MHz ($\eta = 0.16(3)$) appeared at annealing temperatures below 650 °C. Above 650 °C, it was replaced by a second interaction frequency of $\nu_{Q2} = 500(1)$ MHz ($\eta = 0$). The frequencies are attributed to two different carbon–indium pairs. The orientation of the corresponding electric field gradients and the thermal stability of the defect complexes are studied.

1. Introduction

The utilization of carbon in semiconductor technology has begun over the last few decades in combination with other elements and compounds. Carbon plays a vital role in the modification of the properties of semiconductors. Among its many applications important to the present discussion, carbon is used, for instance, to compensate for strain in SiGe compound semiconductors [1]. Apart from deliberate incorporation of carbon into materials, it is also one of the major residual impurities next to oxygen in CZ grown silicon and germanium [2, 3]. Relatively little attention was paid until recently to the formation of the GeC system, because of the very low solubility (10^8–10^{10} cm^{-3}) [4] of carbon in germanium. However, using the electron cyclotron resonance (ECR) plasma processing method Herrold and Dalal [5] were able to grow microcrystalline thin films of germanium carbide on different substrates up to 2% carbon concentration. The newly grown germanium carbide is reported to have an energy bandgap of 1.1 eV, very close to that of silicon, depending on the carbon concentration. This is very important progress towards obtaining crystalline germanium carbide, which has promising electrical and optical properties. Moreover, the implantation technique is also utilized for

doping germanium substrates with carbon [6, 7]. After the recovery of radiation-induced damage, Hoffmann *et al* [6] have observed a significant fraction of the implanted carbon at regular substitutional lattice sites.

In general, there is growing interest in recent years in the investigation of carbon in semiconductors. The perturbed angular correlation (PAC) method has also been employed in an attempt to study carbon in Si, but an In–C pair was not observed for several possible reasons discussed by Ott *et al* [8]. However, using infrared spectroscopy, it was found that indium forms pairs with carbon in Si [9]. Therefore, at first sight an indium–carbon pair is also expected in germanium because of its similar chemical properties to silicon. This could be favoured by the size difference, the carbon atoms compensating for the strain caused by the implantation of the oversized indium atoms into germanium.

In the current work, experiments are conducted using the PAC method to extend the study of the properties of carbon in germanium. In this effort, besides contributing to the understanding of the incorporation of carbon in the host lattice, we present new values of the electric field gradients (EFGs) in the theoretical calculations of isoelectronic impurities in germanium. Carbon is detected at two distinct lattice locations after different annealing temperatures. Discussion on the thermal stability of the defect complexes and comparison with the results of other methods will be made in the following sections.

2. Experimental details

PAC is a nuclear technique, which uses radioactive probe nuclei to extract information about the microscopic environments of the probe atoms. Information about the nature of defects trapped at the probe site can be obtained through the interaction of the nuclear moments of the probe nucleus with the surrounding electromagnetic fields. The probe nucleus ^{111}In is used in all the measurements presented here. The parent nucleus (^{111}In) decays by electron capture and, through successive emission of two γ-rays with energies 171 and 245 keV, to the ground state ^{111}Cd. The intermediate state of the γ–γ cascade has a half-life of $t_{1/2} = 84$ ns, which allows sufficient time for the moment of the intermediate state to interact with external fields before the emission of the second γ-ray in the cascade. The EFG characterizing the defect is the second derivative of the electric potential caused by the surrounding charges. In the principal axes system, the diagonalized field tensor constitutes three components V_{xx}, V_{yy} and V_{zz} with the convention $|V_{xx}| \leqslant |V_{yy}| \leqslant |V_{zz}|$. When the field is entirely produced by charges outside the nucleus then the diagonal elements satisfy the Laplace equation $V_{xx}+V_{yy}+V_{zz} = 0$. Therefore, the EFG can be completely described by two parameters, that is, the main component of the EFG, V_{zz}, and the asymmetry parameter η, defined as

$$\eta = \frac{V_{xx} - V_{yy}}{V_{zz}} \qquad (0 \leqslant \eta \leqslant 1). \tag{1}$$

The quadrupole coupling constant ν_Q characterizing the interaction between the moment of the probe nucleus and the EFG is given by the relation $\nu_Q = eQV_{zz}/h$. Q is the quadrupole moment of the probe nucleus, which has a value of $Q(5/2^+) = 0.83(13)b$ [10] for the isomeric state of ^{111}Cd.

The basic idea of the PAC experiment is the detection of spatially anisotropic γ–γ coincidences, which requires the recording of two different photons γ_1 and γ_2 that can be identified via the different energies E_{γ_1} and E_{γ_2}, respectively. Due to the conservation of angular momentum the emission directions of the γ-rays populating and depopulating the intermediate nuclear state of ^{111}Cd are correlated [10, 11]. This correlation is changed by the interaction between the quadrupole moment of the nucleus in the intermediate state and

extranuclear fields. Hence, such an interaction leads to frequency modulation of the angular correlation pattern. The frequency of modulation is measured by the fast–slow pulse processing technique using four BaF_2 detectors set up situated in a plane at an angle of 90° and 180° with one another. Eight coincidence time spectra ($N(\theta, t)$) are measured at the same time, which contain information about the interaction. From the measured spectra the time differential anisotropy was calculated by the relation $R(t) = 2[N(180°, t) - N(90°, t)]/[N(180°, t) + 2N(90°, t)]$. Finally, a least squares fitting procedure is used to describe the measured $R(t)$ values with a theoretical perturbation function $G_{22}(t)$ [12]. Consequently, the parameters of the quadrupole interaction can be determined by the relation.

$$R(t) = A_{22}G_{22}(t) \tag{2}$$

where A_{22} is the anisotropy constant which depends on the properties of the probe nucleus and the angular resolution of the gamma detectors. Often the probe atoms in the host material are subject to different environments. If there are several distinct sites having fractional populations f_i of the probe nuclei in a unique environment i, the average perturbation function has the form [13]

$$G_{22}(t) = \sum_i f_i G^i_{22}(t), \qquad \sum_i f_i = 1. \tag{3}$$

In general, the time-dependent perturbation function that describes a given interaction can be written as

$$G^i_{22}(t) = \sum_{n=0}^{3} S^i_n \cos(g_n(\eta)\omega^i_0 t) \exp[-g_n(\eta)\omega^i_0 \delta^i t] \tag{4}$$

where the fundamental precession frequency ω_0 of the interaction is defined here as $\omega_0 = (3\pi/10)eQV_{zz}/h$. The value of η can be deduced from the frequency factors $g_n(\eta)$. However, it should be noted that $g_0(\eta) = 0$ to yield the hard core. Moreover, each interaction possesses three transition frequencies ω_1, ω_2 and ω_3. In an axially symmetric field gradient ($\eta = 0$), which corresponds to $g_1(\eta) = 1$, $\omega_0 = \omega_1$ and the remaining components are integer multiples of ω_0, i.e. $\omega_n = n\omega_0$ ($n = 1, 2, 3$). The exponential term δ^i measures the average width of the statistical distribution of the frequency around the mean value. The coefficients S^i_n contain information about the geometry of the EFG with respect to the host lattice [14, 15].

The germanium samples were obtained from a CZ grown germanium wafer with a ⟨100⟩ surface and cut to a size of 6×5 mm^2. The implantations were carried out in two steps: first, ^{111}In was implanted with an energy of 160 keV and a dose between 10^{12} and 10^{13} atoms cm^{-2}. This creates implantation profiles centred at 52 ± 23 nm in Ge, according to the results of the TRIM (transport of ions in matter) simulation program [16]. After the indium implantation the samples were annealed for 600 s at 450 and 600 °C, consecutively. These temperatures were chosen because full recovery from the radiation-induced damage was achieved after this annealing procedure [17, 18]. Then followed an implantation of carbon with a dose of 2.5×10^{15} atoms cm^{-2} and 40 keV. The PAC time spectra were taken successively after each annealing step at temperature T_A in an isochronal annealing program, using the rapid thermal annealing (RTA) method, in a vacuum between 2×10^{-5} and 8×10^{-6} mbar and a holding time 300 s.

3. Results and discussion

After the post-implantation of carbon the spectrum shows a highly disturbed PAC signal. The first sign of recovery of the radiation-induced damage is observed after annealing the sample at 450 °C (see top panel of figure 1). The PAC signal is gradually modulated by an interaction

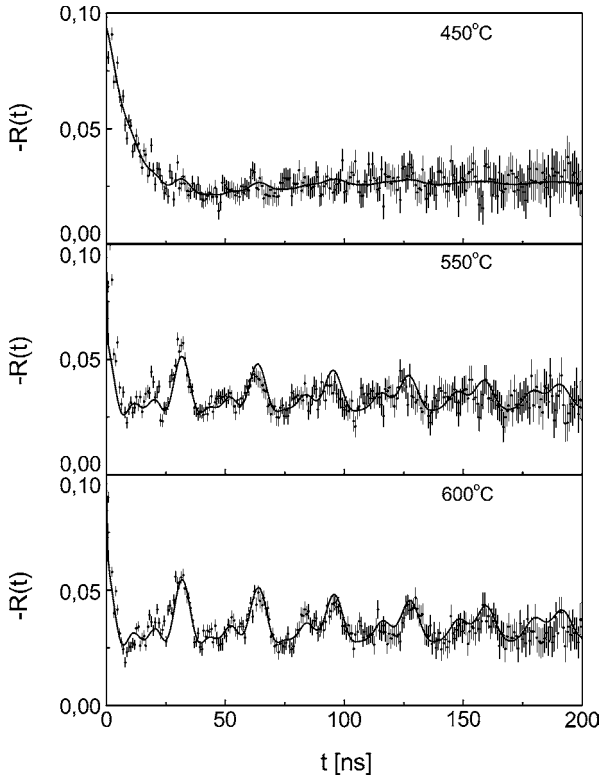

Figure 1. PAC time spectra taken from carbon-doped germanium showing the first interaction frequency of $\nu_Q = 207(1)$ MHz ($\eta = 0.16(3)$), site 1. The full curve is the least squares fit according to equation (2).

frequency of $\nu_{Q1} = 207(1)$ MHz ($\eta = 0.16(3)$). The amplitude of modulation increases with temperature (middle and bottom panels of figure 1), showing the population growth of the probe atom in a unique environment. Besides, the spectra are accompanied by the frequency damping of $\delta_1 = 1.7(6)$ and 1.5(4)% at 550 and 600 °C, respectively. The decreasing tendency of damping with temperature indicates the recovery of damage near the defect complexes. After annealing the sample above 600 °C, this frequency is replaced by another interaction frequency of $\nu_{Q2} = 500(1)$ MHz and ($\eta = 0$) (figure 2), representing a new indium environment. The difference between these two frequencies can be seen from the figures by the various timescales used. The latter dominates the PAC spectra up to 850 °C. Annealing the sample at 900 °C, close to the melting point of germanium, caused a substantial loss of activity of ^{111}In, making further measurements impossible.

In order to identify the orientation of the EFGs with respect to the host lattice, PAC spectra were taken along the three major crystal axes ⟨100⟩, ⟨110⟩ and ⟨111⟩, respectively. The Fourier transforms of the time spectra taken after annealing the sample at 600 °C are given in figure 3. They show distinctly separated amplitudes for the three transition frequencies (ω_1, ω_2 and ω_3) associated with the quadrupole interaction frequency (QIF) ν_{Q1} (site 1). In all three crystal axes orientations, the amplitude of the first transition ω_1 remains dominant (see figure 3). However, when the detectors are positioned along the ⟨111⟩ crystal axis the amplitudes of ω_2 and ω_3 almost vanish. This indicates the alignment of V_{zz} in the direction of the detectors. The same results are observed for the second interaction frequency $\nu_{Q2} = 500(1)$ MHz (site 2) [18].

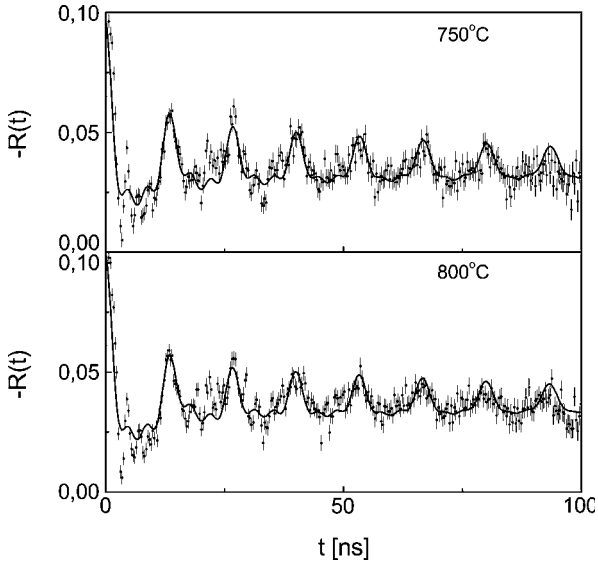

Figure 2. PAC time spectra of the In–C pair after annealing the sample above 650 °C, it shows the second interaction frequency of $\nu_Q = 500(1)$ MHz ($\eta = 0$), site 2.

Therefore, in both cases the principal component of the EFGs present at the site of the probe atoms are oriented along the ⟨111⟩ crystal axis.

The fractional population of the probe atoms at lattice sites in the range of annealing temperatures between $T_A = 450$ and 800 °C is shown in figure 4. Below $T_A = 450$ °C no unique interaction frequency is observed. The spectra can be described by a broad frequency distribution characteristic for probe atoms in non-unique sites due to implantation-induced lattice damage. At $T_A = 450$ °C, 16(2)% of the probe atoms are detected in an undisturbed cubic environment, EFG = 0 (site 0 of figure 4). Such a vanishing EFG is expected for ^{111}In in regular substitutional sites of the cubic Ge lattice. This fraction grows at higher annealing temperatures as the sample recovers from radiation-induced damage, but its population gradually changes by the formation of various complexes in the sample. Besides, another 10(2)% of the probes are found simultaneously in the new environment (site 1 of figure 4). This site is populated to a maximum of $f_1 = 34(2)$% after annealing the sample at 600 °C. The fraction decreases at higher temperatures and eventually disappears at $T_A = 700$ °C. When the depopulation of site 1 begins above $T_A = 600$ °C, a new interaction frequency representing a different indium environment (site 2) is evolved. The population of site 2 increases rapidly with annealing temperature, and grows to a maximum of $f_2 = 35(3)$% at $T_A = 750$ °C. The remaining fraction, not given in figure 4, is due to probe atoms in non-unique lattice sites. Above $T_A = 450$ °C, the best fits to the data are obtained by assigning $f_p = 48(5)$% of the probes to lattice sites with highly disturbed environments. These sites could be attributed to the ^{111}In in carbon clusters or carbon stabilized defects.

According to the infrared absorption and ion channelling studies of carbon in germanium [6], which will be discussed later in comparison with the current results, a significant fraction of substitutional carbon is reported in the range of annealing temperatures from 350 to 700 °C. Another lattice location of carbon at high temperatures was not indicated by these methods. The interaction of a ^{111}In acceptor with defects (vacancies, self-interstitials) and group V donors in Ge has been studied previously by several groups [19, 20], employing

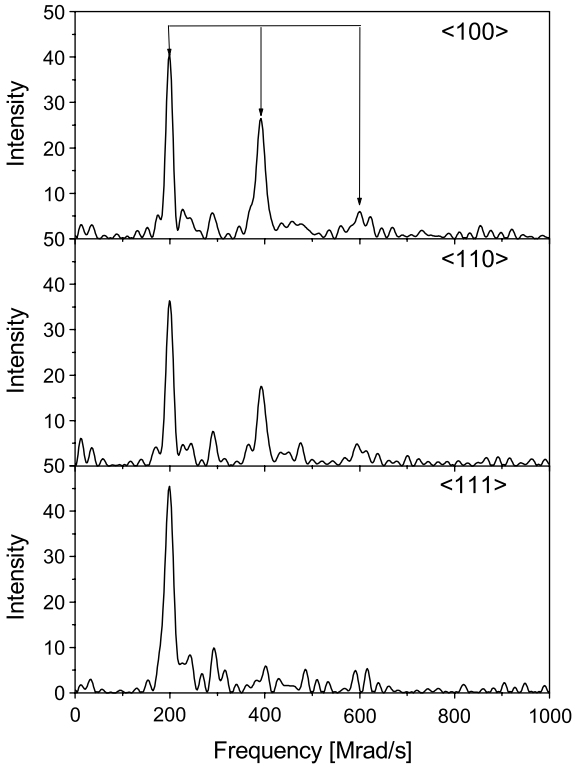

Figure 3. Fourier transform of the PAC time spectra taken at three major crystal axes, as indicated in the panels, after annealing the sample at 600 °C. It represents the first interaction frequency of $\nu_Q = 207(1)$ MHz.

the PAC method. In all cases, unique QIFs have been found and could be assigned to the In-defect and In-donor pairs. The In-defect pairs show a relatively low binding energy and break up already below $T_A = 160\,^{\circ}\mathrm{C}$, but, the In-donor pairs tend to be more stable well above $T_A = 600\,^{\circ}\mathrm{C}$. The QIFs found in the present measurements after the implantation of carbon have not been detected in any of the previous investigations. Hence, it can be concluded that both frequencies, which are observed above $T_A = 400\,^{\circ}\mathrm{C}$, are due to the trapping of carbon at the ^{111}In probe atom. Besides, the structures of the complexes can be derived from the measured hyperfine interaction parameters.

Therefore, based on the orientation of the EFG along the $\langle 111 \rangle$ crystal axis and channelling information on substitutional carbon in germanium, the first QIF of $\nu_{Q1} = 207(1)$ MHz is assigned to the interaction of a substitutional indium–carbon pair. Normally, the EFG tensor resulting from a substitutional indium–impurity pair in germanium is axially symmetric about the $\langle 111 \rangle$ crystal axis. However, the existence of the asymmetry parameter ($\eta = 0.16(3)$) at site 1 suggests that carbon is not in a perfect substitutional site in germanium. But, it could have taken a near-substitutional position, which leads to a change in the symmetry of the charge distribution around the probe nucleus. This is consistent with the estimated 0.2 Å displacement of carbon from the regular lattice site measured by ion channelling [6]. The observed asymmetry in this work can also be regarded as the relaxation of carbon towards either $\langle 100 \rangle$, $\langle 110 \rangle$ or a combination of both axes, and thus breaking the ideal $\langle 111 \rangle$ symmetry axis of the EFG tensor. It is difficult to assign the exact location of relaxed substitutional carbon

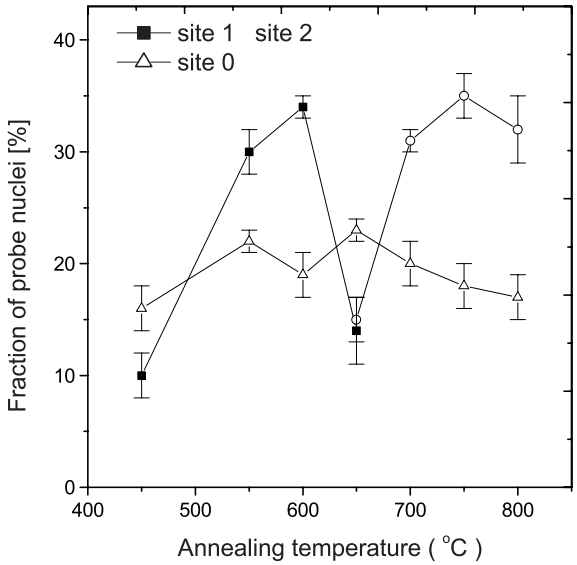

Figure 4. The fractions of the probe nuclei subject to various environments in carbon-doped germanium. Site 1 and site 2 are complexes associated with indium and carbon. Site 0 represents the fraction of undisturbed substitutional probe atoms.

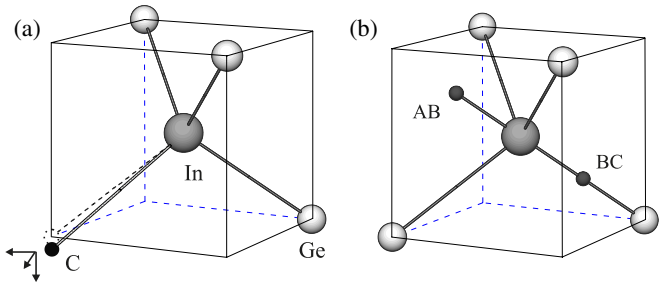

Figure 5. The indium environments, where carbon takes alternately different lattice sites in germanium. (a) Substitutional site showing one possible relaxation direction (site 1), (b) interstitial sites (site 2).

(This figure is in colour only in the electronic version)

based on merely the magnitude of η and the orientation of the EFG. Nevertheless, figure 5(a) shows one possible relaxation direction that can lead to a change in the symmetry of the EFG. The reason for such relaxation could probably be the presence of a high concentration of impurity atoms in the host lattice. In fact, it has been reported by Kaufmann [21] in the past that the incorporation of impurity in group IVB metals could lead to non-zero values of η. Therefore, in germanium crystal the undersized carbon pulls the nearest host atoms in the effort to form sp^3 hybridized covalent bonds, whereas the oversized indium pushes its neighbours outward, creating oppositely strained environments at two ends of the In–C bond. The In–C bond under such strained conditions could lie slightly away from the normal symmetry axis, causing the non-zero asymmetry parameter. Furthermore, this relaxation must be very small so that the orientation of V_{zz} remains close to the $\langle 111 \rangle$ crystal axis, as observed in the experiment.

The second frequency (site 2) is most likely a pair of substitutional indium and interstitial carbon. Other possibilities, such as more than one substitutional C atom around a probe nucleus, are not impossible, but less probable because of the significant difference of the bond lengths of carbon (1.55 Å) and germanium (2.45 Å) [22]. Moreover, the measured asymmetry parameter ($\eta = 0$) from this site leaves even a two C cluster at regular sites next to an indium out of the question, because two substitutional nearest neighbours to the probe atom in the diamond lattice usually result in a non-zero asymmetry parameter. On the other hand, the measurements taken at (0.45, 2.5 and 4.5) $\times 10^{15}$ atoms cm^{-2} doses of carbon on various samples show no indication of the dependence of the population of this complex on the concentration carbon, at least in the chosen dose range. The absence of additional frequency, in the temperature interval where site 2 is detected, and the non-dependence of the complex on carbon concentration suggests a less probable occurrence of two interstitial carbons at a probe site. Therefore, the location of carbon at high annealing temperatures would likely be either a bonding or anti-bonding interstitial centre (figure 5(b)).

Frequency damping is generally large in all the spectra taken after carbon implantation. Damping values $\delta_1 = \delta_2 = 1.5(2)\%$ are obtained at $T_A = 600$ and 750 °C, respectively. This is evident in the figures (see figures 1 and 2) by decreasing amplitudes of modulation with time. Frequency damping is believed to be the result of radiation damage caused by ion implantations. However, its presence even at high annealing temperatures (up to $T_A = 800$ °C) suggests that the sample has not completely recovered from the damage, or it has sustained permanent surface deformation. Carbon implantation is not expected to cause permanent damage at the chosen implantation parameters, but during crystal regrowth dense dislocation loops can be formed in the sample because of the lattice mismatch between the different atoms involved. The In–C complex could take sites near the edge of such dislocations where lattice constants are different from the pure Ge crystal. It can also be formed far from the dislocations. Hence, the non-uniform environment of the same complexes would result in a wide statistical distribution of the EFG around the mean value, causing a frequency damping in the time spectra. Moreover, the presence of a substantial fraction of the probe atoms in an undefined lattice location is also an indication of the complex nature of carbon-implanted germanium crystal.

Preliminary experimental tests show that the observed complexes are not reversible after dissociation at $T_A = 650$ and 800 °C, respectively. Therefore, based on first-order kinetics, the dissociation energies of the complexes are estimated to be 2.84 and 3.52 eV for substitutional and interstitial carbon in germanium, respectively. These values are according to the relation.

$$E_d = kT \ln\left[\frac{1}{t\nu}\ln\left(\frac{N_0}{N}\right)\right] \tag{5}$$

where the ratios N_0/N are obtained from the initial and final fractional population of the complexes after annealing the sample at temperature T for time t. The parameter ν is a dissociation attempt frequency, which is assumed here as 10^{13} s^{-1} [23]. The difference in the dissociation energies is obviously the result of the various energies required to form substitutional and interstitial carbon. These values are not unreasonable compared to the energies ~2.8 and ~4.7 eV required to break the Ge–Ge and Ge–C bonds, respectively [6]. Besides, the In–C complexes discussed here involve the atoms In, Ge and C, which have different thermodynamic properties than the Ge–C system.

An interesting similarity is observed in the population of substitutional carbon in PAC on the one hand, and ion channelling and infrared absorption methods on the other [6]. According to the latter, substitutional carbon is observed after annealing the sample above $T_A = 350$ °C; it is depopulated from this site at high temperatures and eventually disappears at $T_A = 700$ °C.

Table 1. Summary of the results.

Complexes	ν_Q (MHz)	η	Max. fraction (%)
Site 1	207(1) (at 21 °C)	0.16(3)	34(2)
Site 2	500(1) (at 21 °C)	0.0	35(3)

The report also indicated that a maximum 31(3)% of the implanted carbon was found at substitutional lattice sites while the remaining 69(3)% are randomly located. In PAC, an indium–carbon complex (site 1) is detected below 650 °C annealing temperatures. The largest population of this complex is 34(2)% of the probe atoms (table 1). Therefore, comparing the ranges of temperature, the substitutional carbon is observed by ion channelling and infrared absorption on the one hand and the detection of site 1 by PAC (figure 4) on the other. We found similar ranges, in which all three methods are able to detect the occurrence of well-defined structural sites of carbon in germanium. According to this information, it is possible to conclude that site 1 with an interaction frequency $\nu_{Q1} = 207(1)$ MHz is the result of the interaction of indium with substitutional carbon in germanium. Despite the limitation of PAC to only the population of the probe atoms, the present results also show the existence of substantial amounts of isolated substitutional carbon below $T_A = 650$ °C. Moreover, the observation of no substitutional fraction of carbon in Ge above $T_A = 650$ °C by the ion channelling method suggests that site 2 in the current measurement is not a consequence of the interaction of indium with substitutional carbon, as indicated in the above discussion.

The ratio of the quadrupole coupling constants of the two complexes yields $\nu_{Q1}/\nu_{Q2} = 0.414$. Based on the point charge model, assuming interstitial carbon carries charge twice that of substitutional carbon, the ratio of the proximity of carbon to indium at the interstitial and the substitutional sites is $r_i/r_s = 0.9$. This is, of course, far from expected unless interstitial carbon occupies anti-bonding sites instead of bonding (figure 5). This result clearly shows the inadequacy of the model, which makes it difficult to derive the exact interstitial position of carbon from the measured data. However, the r^{-3} dependence of the EFG and the fact that the magnitude of the EFG of site 2, about two times larger than that of site 1, suggests that carbon at site 2 is in closer proximity to the indium than site 1. Therefore, the most probable location of site 2 by this comparison is once again an interstitial.

4. Conclusion

Two interaction frequencies are detected for the first time after high dose carbon implantation in germanium. The frequencies are associated with indium–carbon pairs, where carbon alternately takes substitutional and interstitial lattice sites at different temperatures. The orientations of the resulting EFGs lie along the ⟨111⟩ crystal axis. Significant populations of isolated substitutional carbon are observed below 650 °C annealing temperatures. However, the majority of the implanted carbon possesses disordered lattice sites, where nearly 50% of the probe atoms are trapped. The reported properties of substitutional carbon in germanium by ion channelling and infrared spectroscopy are in good agreement with the behaviour of site 1.

Acknowledgment

The authors are grateful to the German Academic Exchange Service (DAAD) for the financial support that they received during this work.

References

[1] Eberl K, Iyer S S, Zollner S, Tsang J C and LeGoues F K 1992 *Appl. Phys. Lett.* **60** 3033
[2] Haller E E, Hansen W L, Luke P, McMurray R and Jarrett B 1982 *IEEE Trans. Nucl. Sci.* **29** 745
[3] Newman N C 1982 *Rep. Prog. Phys.* **45** 1163
[4] Scace R I and Slack G A 1959 *J. Chem. Phys.* **30** 1551
[5] Herrold J T and Dalal V L 2000 *J. Non-Cryst. Solids* **270** 255
[6] Hoffmann L, Bach J C and Nielsen B B 1997 *Phys. Rev.* B **55** 11167
[7] Yamaguchi S, Fujino Y, Naramoto H and Ozawa K 1989 *Nucl. Instrum. Methods* B **39** 409
[8] Ott U, Wolf H, Krings Th, Wichert Th, Häßlein H, Sielemann R, Deicher M, Newman R C and Zulehner W 1994 *Mater. Sci. Forum* **143–147** 1251
[9] Jones C E, Schafer D, Scott W and Hager R J 1981 *J. Appl. Phys.* **52** 5148
[10] Schatz G and Weidinger A 1996 *Nuclear Condensed Matter Physics* (New York: Wiley)
[11] Frauenfelder H and Steffen R M 1965 *Alpha, Beta-, Gamma-Ray Spectroscopy* vol 2, ed K Siegbahn (Amsterdam: North-Holland) p 997
[12] Barradas N P, Rots M, Melo A A and Soares J C 1993 *Phys. Rev.* B **47** 8763
[13] Arends A R, Hohenemser C, Pleiter F and De Waard H 1980 *Hyperfine Interact.* **8** 191
[14] Wichert Th, Deicher M, Grübel G, Keller R, Schulz N and Skudlik H 1989 *Appl. Phys.* A **48** 59
[15] Wegner D, Schröder H and Lieb K P 1984 *Radiat. Eff. Lett.* **85** 13
[16] Ziegler J F, Cole G W and Baglin J E E 1972 *Appl. Phys. Lett.* **21** 177
[17] Marx G and Vianden R 1995 *Phys. Lett.* A **210** 364
[18] Tessema G 2003 *PhD Dissertation* Helmholtz Institut für Strahlen- und Kernphysik, University of Bonn, Germany
[19] Feuser U, Vianden R and Pasquevich A F 1990 *Hyperfine Interact.* **60** 829
[20] Forkel D, Achtziger N, Baurichter A, Deicher M, Deubler S, Puschmann M, Wolf H and Witthuhn W 1992 *Nucl. Instrum. Methods* B **63** 217
[21] Kaufmann E N 1973 *Phys. Rev.* B **8** 1382
[22] Dean J A (ed) 1979 *Lange's Handbook of Chemistry* (New York: McGraw-Hill) pp 3–121
[23] Skudlik H, Deicher M, Keller R, Magerle R, Pfeiffer W, Pross P, Recknagel E and Wichert Th 1991 *Phys. Rev.* B **46** 2172